JCSE The Journal of Corrosion Science and Engineering
ISSN 1466-8858 Volume 12, Preprint 14 submitted 13 May 2009

DYNAMIC STUDIES ON THE INHIBITIVE ACTION OF MAGNESIUM HYDROXIDE ON HOT ASH CORROSION IN A KEROSENE FIRED FURNACE.

M. M. Barbooti, S. Al-Niaimi, AND, K.F. Al-Sultani,
School of Applied Sciences and Department of Chemical Engineering, University of Technology, Baghdad, Iraq.
*Present Address: Department of Material Engineering, College of Engineering, University of Babylon, Hilla, Iraq.

ABSTRACT

The inhibitive effect of magnesium oxide on the hot ash corrosion of steel structures of power generation station was studied using a kerosene fired furnace. Three alloys were selected including [SA 178A, 209 T1, 213 T11], prepared as rectangular pieces from water wall tubes and superheater tubes of a local power station. The heating chamber of the furnace had shelves on which specimens are placed. $Mg(OH)_2$ was mixed with synthetic slag (67%wt V_2O_5 and 33% wt Na_2SO_4) at molar ratios of 1:1, 1:2 and 1:3, respectively and applied on the surface of the cleaned specimens. The tests were carried out at fixed (4 h) and various time intervals (2-10 h) to study the normal oxidation at various temperatures (550-950˚C). The rate of oxidation is accelerated in the presence of vanadic slag and resulted in increased corrosion rate with increasing temperature (550-950 ºC). X-ray diffraction indicated the formation of NaV_3O_8, $Na_2O.V_2O_4.5V_2O_5$, $Na_4V_2O_7$, $VOSO_4$, Na_2SO_4 and iron oxide (Fe_2O_3) . The weight loss of the three alloys specimens indicated a Clear reduction in the degree of corrosion with increasing $Mg(OH)_2$ content. The scale changed into a powder form which can be easily removed from the surface of the specimens. The best results were obtained with the mole ratio 3:1, which gave inhibition efficiency of 85% at 550°C. The inhibition efficiency increases with

ISSN 1466-8858 Volume 12, Preprint 14 submitted 3 May 2009

temperature decrease. With the introduction of $Mg(OH)_2$ with the ash magnesium vanadate $Mg_3V_2O_8$ was a major constituent together with some MgO.

KEY Words: Magnesium Hydroxide, Hot Ash corrosion, Inhibition.

INTRODUCTION

Singh et al recently reviewed the coupled action of sodium sulfate and vanadium pentoxide on the corrosion of iron and nickel superalloys in power generation stations. They concluded that It is basically induced by the impurities such as Na, V, S, *etc.* present in the coal or in fuel oil used for combustion in the mentioned applications[1]. Ash fouling and flame-side corrosion of metal surface, together with heat transfer surface fouling are major problems in power generation stations when burning heavy oils. Vanadium occurs in the form of porphyrinic and non-porphyrinic in crude oils [2]. These compounds decompose in the gas stream to give mainly vanadium pentoxide (V_2O_5), which is most damaging due to its low melting point (690°C) i.e. it is in its liquid state at normal combustion temperature. Sodium in the oil is mainly present as (NaCl) and is readily vaporized during the combustion process [3]. The presence of a liquid phase on the surface of a metal is usually necessary for corrosion reactions to occur at high rates. The most likely liquid phases are based on vanadium pentoxide and sodium sulphate complexes depending upon the exact analysis of the fuel used [4]. A series of compounds are formed between (Na_2O) and (V_2O_5), some of which have melting points below the operating temperature of boilers and turbines. The eutectic formed between ($5Na_2O.V_2O_4.11V_2O_5$) and sodium metavanadate ($Na_2O.V_2O_5$) melts at (527°C). However, under an

ISSN 1466-8858 Volume 12, Preprint 14 submitted 3 May 2009

atmosphere containing oxides of sulphur, other components can form e.g. Na_2SO_4, $Na_2S_2O_7$, V_2O_5. $2SO_3$ and V_2O_5.1/2 SO_3 [5].

Prevention of hot ash corrosion is impossible and a reduction can be effectively performed. In contaminated combustion atmospheres, there are three basic ways to reduce the corrosion problems and these are:-

I-Removal of harmful impurities presents in the environment.

II-Addition of a compound to counteract the harmful impurities .

III-Changing the combustion condition to minimize attack.

Combustion Control can be done to minimize corrosion problems in boilers and turbines. The use of water-in-oil emulsions (in which each fuel droplet leaving the atomizer contains a number of micro-droplets of water) is a promising technique to reduce smoke and (NO_x) emissions from boilers and gas turbines. Other possible benefits include the reduction in excess air with consequent reduction in SO_3 formation and the elimination of metal-containing antismoke additives and the resulting deposits and fouling in gas turbines, the ability to use heavier and cheaper fuel [6].

The use of corrosion resistance coatings for existing alloys has found widest application in the gas turbine and boiler field. Metallic coating has been applied by electrodeposition, high temperature diffusion and plasma are spraying. The effect of ceramic coatings has also been investigated. The metallic coatings examined were principally those of silicon, chromium, aluminum, zirconium and beryllium [7]. The higher the chromium content of the alloy, the better would be the hot-corrosion resistance [4]. El-Dahshan [8] observed that Co-Cr-W alloys were more resistant to oxidation than (Ni-Cr-W) alloys when coated with sodium sulphate.

ISSN 1466-8858 Volume 12, Preprint 14 submitted 3 May 2009

The corrosive effect of ash-causing contaminants, principally vanadium and nickel can be neutralized by chemical additives. The additives work by forming a stable vanadate of higher melting point than the vanadium compounds originally present, thus preventing formation of a liquid phase at the operating temperature [9, 10]. Macfarlane [4], reviewed the effect of such additives in particular calcium, magnesium and zinc compounds. Magnesium additions, however, raise the melting point of the deposit appreciably from 680°C for $1/2MgO.V_2O_5$ to 1100°C for $3MgO.V_2O_5$ and have been fond to be very effective.

$$3MgO + V_2O_5 \longrightarrow Mg_3V_2O_8 \text{ ……...(1)}$$

The $Mg_3V_2O_8$ is solid at the operating temperature of industrial boiler tubes and turbine blades [11, 12]. When sufficient SO_3 is present, MgO can be sulphated to $MgSO_4$, which can then react with V_2O_5 to from magnesium pyrovanadate which may be molten on the surface boiler tuber and turbine blades [3].

$$MgSO_4 + V_2O_5 \longrightarrow 2MgO.V_2O_5 + SO_3 \text{ ……..……(2)}$$

Thus, corrosion control in low grade or residual fuel oils is modified by the presence of (SO_3) [13]. Blauenstein [14] injected dispersed magnesia additive and could gain benefits on a 300 MW oil-fired boiler such as improved combustion, reduction in total particulate emissions and reduction in metallic corrosion as indicated by higher pH ash and confirmed by iron determinations on the ash. An ideal additive should be miscible with fuel oil and improve combustion conditions, especially atomization.

Barbooti et al. studied the inhibitive action of magnesium oxide and magnesium sulphate [15] on the hot ash corrosion by heating alloy specimens in an electrical furnace and following the inhibition by weight loss and chemical analysis of the scale. Nishikawa et al [16] have studied the effect of Mg-Additive against high temperature fouling and corrosion. When Mg was added,

ISSN 1466-8858 Volume 12, Preprint 14 submitted 3 May 2009

weight loss due to high temperature corrosion was reduced to about equal level of corrosion by clean kerosene firing in the temperature range below 700°C.

The present work is a dynamic study of the action of magnesium hydroxide ($Mg(OH)_2$) as an inhibitor of hot ash corrosion using a pilot scale kerosene fired furnace.

EXPERIMENTAL

Materials and Chemicals

Three alloys were selected from those used in boilers including: SA 178A, 209 T1 and 213 T11 (water wall tubes and superheater tubes) from South-Baghdad Power Station. The chemical composition of the alloy used in this work is shown in Table 1[17]. Magnesium hydroxide was supplied by a local factory, with a purity of 98.5%.

Heating Furnace:

A kerosene fuelled furnace was designed especially for this study with ceramic shelves. Fig. 1 shows the heating chamber during work, where the shelves on which specimens are placed are shown.

Procedures

The Specimens Preparation

The specimens were cut from the pipes into rectangular pieces (5x10x20 mm) (W x L x T) and mechanically polished with emery paper (100, 320, 600 and 1000) under running tap water and rinsed with distilled water, benzene, then these specimens were dried and left in a vacuum desiccators and weighed.

The vanadic slag chosen for this work was based on 67%wt (V_2O_5) and 33% wt (Na_2SO_4). This mixture was chosen because it has been shown to be the most representative corrosive simulated by other workers [18, 19]. Weighed

ISSN 1466-8858 Volume 12, Preprint 14 submitted 3 May 2009

proportions of V_2O_5 and Na_2SO_4 in the ratio 3:1 were mixed and ground in an agate mortar for 15 minutes. The slag mixture was than stored in desiccators until required for use.

About 2.09 g of magnesium hydroxide $Mg(OH)_2$ was mixed with and 10 g synthetic ash and homogenized with 3 mls of acetone. With the aid of a syringe the mixture was applied onto the surface of the cleaned specimens to give a coating of 1 mole $Mg(OH)_2$: 1 mole ash. The tests were carried out at various time intervals (2, 4, 6, 8 and 10 h) to study the normal oxidation at different temperature (550, 650, 750, 850 and 950 ˚C). Constant time tests involved heating at the specified temperatures for 4 h. At the end of the run, the furnace is switched off and samples are taken out after 24 h. The specimens are dipped in caustic soda solution containing zinc dust (20% NaOH + 200g Zn/L.), at 60˚C for five minutes, and abraded with emery paper grades (100, 320, 600 and 1000) respectively under running tap water, then rinsed with water and kept over silica gel for one hour, and finally weighed to the fourth decimal.

Analysis

The specimens exposed were examined in detail, particular notice being given to the color and appearance of corrosion products and the extent of spallation. The X-ray diffraction technique was used to identify the scale compounds and the corrosion products formed in this work using Phillips X-ray Difractometer, Type PW1050 Holland with iron target to produce an x-ray beam of wavelength of Fe-kα at 1.93 Å using a tube current of 20 mA. and a voltage of 40KV. The speed scans of [2°(20)/1cm]. Reference was made to the ASTM card Index.

RESULTS AND DISCUSSION

Effect of Vanadic Slag:

Fig. 2 shows the dependence of weight gain with temperature after 4 h exposures time. The rate of oxidation is accelerated in the presence of vanadic

ISSN 1466-8858 Volume 12, Preprint 14 submitted 3 May 2009

slag mixture in comparison with uncoated specimens. Further, the application of this slag on the specimen surface resulted in increased corrosion rate with increasing temperature (550-950 °C). The scale formed after the thermal treatment is sticky and metallic in color. The X-ray diffraction analysis indicated the formation of sodium vanadate which is the most important aggressive species in the (Na-V-O) system. This product became appreciable after the melting of the eutectic mixture and increase with temperature. Therefore, Na_2SO_4, which has no individual aggressive behavior towards the metal, facilitates the low temperature melting of the ash and initiates the formation of sodium vanadate, which attacks the metal surfaces [4].

At 850˚ C, the weight gain for (SA-178A) in a (V_2O_5 : Na_2SO_4) slag is 0.16 kg/m^2 compared with 0.013 kg/m^2 for normal combustion for the non-coated specimens. This indicates high corrosion behavior occurring at (850 ˚C) because (V_2O_5 – Na_2SO_4) system melts at about (650 ˚C) and forms highly corrosive sodium vanadates [18, 19]. For example, after (4h) and (850˚C), the average weight gain for (213 T1) in a V_2O_5:Na_2SO_4 mixture is 0.14 kg/m^2 compared with 0.011 kg/m^2 for specimen non-coated.

The relation between the heating intervals and the weight gain at different temperatures is typically shown in Figs 3 and 4. It is clear that the increase in time, leads to increase in weight gain and hence vanadic slags highly accelerated the oxidation of the alloys. Much of the weight gain occurred within the high temperature regions (750, 850 and 950 ˚C) because many sodium-vanadium bronzes such $NaVO_3$, $Na_2O.V_2O_5$, $Na_2O.3V_2O_5$, $Na_2O.6V_2O_5$ and $Na_2O.V_2O_4.5V_2O_5$ are predominant above (650 ˚C). These catastrophically oxidize the alloy components acting as oxygen carriers, metal oxide distorts, or dissolving agents of the protective oxide layer, and this leads to an accelerated increase in weight gain with temperature rise [19]. The figures clearly show that

ISSN 1466-8858 Volume 12, Preprint 14 submitted 3 May 2009

the increase in exposure time gives increase in weight gain for all specimens coated with slag and those non-coated.

Effect of $Mg(OH)_2$ Addition

Figs. 5 and 6 show the weight loss of the three alloys specimens coated with $Mg(OH)_2$ and slag at mole ratio of 1:1 , 2:1, and 3:1, respectively. Clear reduction in the degree of corrosion with increasing $Mg(OH)_2$ content can be seen. The color of the scale changed from brown-yellow to red. The best ratio from $Mg(OH)_2$: Ash is 3:1 because the mixture on the surface of specimens was become totally from the rest of the specimens where the coating turned into a white powder that is easily removed by simple tapping of the specimen. This ensures that with a magnesium addition three times the amount of vanadium, a high melting material is produced [20, 21].

The results are given in Tables 3-7. The optimum $Mg(OH)_2$:Ash ratio is 3:1, which gave inhibition efficiency of 85% at 550°C. The results indicate that the inhibition efficiency increases with temperature decrease. The best value is obtained at a temperature of 550 ˚C.

X-Ray Diffraction Analysis

For (SA-178A) alloy, the constituents of the coating or the scales of the corroded specimens were identified by X-ray diffraction analysis. Fig. 7 shows the diffraction pattern of the scale resulted from the synthetic ash after heating at (750°C) for (4h). The main peaks of sodium vanadates $NaVO_3$ at 2.799Å and α-$NaVO_3$ at 2.097 Å could be identified together with ferric oxide at 3.66 Å. This is an indication of the role of molten sodium vanadate on introducing oxygen to react with the iron surface so that it catalyzed the oxidation of the metal [22]. Furthermore, the in situ formed oxide dissolves in the molten layer of the ash compounds and causes the gradual depletion of iron.

ISSN 1466-8858 Volume 12, Preprint 14 submitted 3 May 2009

For the 209 T1 alloy the effect of ash on the iron surface confirmed the oxidation and dissolution of Fe_2O_3 in the molten scale in addition to the formation of several types of sodium vanadates. The sodium- vanadium bronzes, namely: NaV_3O_8 at 6.508, 3.58 and 2.593Å, $Na_2O.V_2O_4.5V_2O_5$ at 3.338 Å, $Na_4V_2O_7$ at 4.08 and 2.298 Å. The thermal treatment also resulted in the formation of vanadyl sulfate ($VOSO_4$ and its main peaks at 5.017, 2.107 and 1.981 Å predominate at the diffraction pattern (Fig.8). Similarly residual sodium sulfate could be identified, Na_2SO_4 (1.572 Å) and iron oxide (Fe_2O_3) at 3.769 Å.

With the introduction of magnesium hydroxide $Mg(OH)_2$ and ash, at 1:1 mole ratio, the diffraction pattern indicated a clear diminishing of the main peaks of sodium vanadates (mainly the 3. 477 Å peak) accompanied by the appearance of same new peak related to magnesium oxide (2.105 Å) and magnesium vanadate (2.677 and 1.744 Å). However magnesium sulfate also showed up at 1.972 Å. Thus, magnesium competed well with sodium to abstract the vanadium and consequently prevented its aggressive effect towards iron and other constituents of the SA-178A alloy.

Further increase of magnesium hydroxide up to (2: 1) confirmed the inhibition efficiency where the diffraction pattern was simpler than that related to the sodium scale since no sign for sodium vanadate could be identified regarding the 213-T11 alloy. Magnesium vanadate $Mg_3V_2O_8$ was a major constituent and the peaks related to it could well be resolved (3.38, 3.28 and 3.026 Å). Again, MgO was present in the studied sample (2.10 Å).

To ensure better corrosion prevention, a third additive to ash mixture was used which is the 3:1 ($Mg(OH)_2$:Ash) . The X-ray diffraction–patterns of the coating of the three alloys heated for 4 h at 850 C° can be seen in Fig. 9. It is apparent that MgO peak predominates at the three samples indicating that no further increase in $Mg(OH)_2$ content is necessary. Besides, the patterns did not show

ISSN 1466-8858 Volume 12, Preprint 14 submitted 3 May 2009

significant signs for the sodium vanadates, i. e. any chance for the vanadium to from corrosive material with sodium.

Consequently, magnesium vanadates existed in the three samples as indicated by the main diffraction peaks at 5.78, 3.20, 3.043, 3.036, 2.618, 2.582, 1.744, 1.743 and 1.701 Å. Thus, the inclusion of magnesium in the coating completely inhibited the formation of the aggressive sodium vanadyl vanadates and formation of the high melting species, the magnesium vanadate instead [16, 22 and 23].

CONCLUSIONS

Magnesium hydroxide can be successfully used for the prevention of hot ash corrosion of steel structures of power generation stations. The optimum efficiency of inhibition could be attained at 3:1 molar mixture of $Mg(OH)_2$: synthetic ash. The study of inhibition can well be carried out in a kerosene fired furnace to simulate the dynamic nature of the process. X-ray diffraction analysis indicated complete diminishing of the formation of the aggressive sodium vanadates and the formation of the high melting magnesium vanadate which can be easily removed from the surface of the steel pipes and other parts of the boilers.

REFERENCES

1. H. Singh, D. Puri and S. Prakash, "An overview of Na_2SO_4 and/or V_2O_5 induced hot corrosion of Fe- and Ni-based superalloys, Rev. Adv. Mater. Sci. 16 (2007) 27-50
2. M. M. Barbooti, E.Z. Said, E.B. Hassan and S.M. Abdul-Ridha, Fuel, 68 (1989) 84-87.
3. D.M. Johnson, D.P. Whittle and J. Stringer, Corrosion Sci., 721 (1975) 15.

4. N. Birks, G.H. Meier and F. S. Pettit, "Introduction to the High Temperature Oxidation of Metals", 2nd Ed., Cambridge, 2006.
5. P.G. Kristensen and A. Bentkarll, Combust. Sci. Technol., 157 (2000) 263.
6. K. B. Alexander, K. PruBner, P.Y. Hou and P.T. Tortorelli, in "Microscopy of Oxidation",. J.B. Newcomb and J.A. Little Eds., The Institute of Metals. 1997, Chap. 3, pp 246-255.
7. K. Page, and R. J. Taylor, in A. B. Hart, and A.J. Cutler, Eds., "Deposition and Corrosion in Gas Turbine", Applied Science, London, 1973, P 350.
8. M. E. EL- Dahshan, Proc. 1st Arab Conf. Corrosion, Kuwait, 1987, PP 347-361.
9. R.A Rapp, Pure and Appl. Chem., , 62 (1990), No. 1.
10. Petrolite Corp., Tretolite Div., "Fuel Addition", Petrolite. 1986.
11. J. R. Rhys-Jones, T.N. Nicholils and P. Hancock, P., Corrosion Sci., , 23 (1983) 39-44.
12. J. Stringer, "High Temperature Corrosion Issues in Energy-Related Systems", Materials Research, , 4l7 (2004) 1-9.
13. P. Hancock, Corrosion Sci., , 23 (1982) No.51.
14. E. Blauenstein, Engineering found. Conf., New England College, New Hampshire, July-26 , 1977.
15. M.M. Barbooti, S.H. AL-Madfai and H. J. Nassonri, Thermochim. Acta., 1988, 126, 34-49.
16. E. Nishikawa, M. Kaji and S. Ishigai, Proc. ASME, JSME Therm. Eng. Conf., 1 (1983) 545-52.
17. R. Francois, L. Thiorry and L. Benoit, "Piping Equipment / Materials Petrole", Trouvay and Cavrin, API, ASTM, ASME Standard, 1998.

18. H.C. Child, "The Effect of composition of Gas Turbine Alloys on Resistance of Scalling and Vanadium Pentoxide", J.I.S.I., 1985.
19. M. M. Barbooti, Proc. 1st. Conf. Chem. Petrochem. Ind. (Chem-Arab), Beirut, 2001, 10-14 Jan.,
20. R.C. Kerby and J.R. Wilson, Engineering for Power, ASME-Trans., Vol. 1, 1973.
21. A.V. Malik, and S. Ahmed, British Corrosion J., 20 (1985) 181.
22. J. A. Fellows, Metals Handbook, "Fractograph and Atlas of Fractographs", ASM Handbook Committee, 8th Edition, 1974, Vol.9.
23. K.H. Andersen and J. Fleming, Energy Fuels, 14 (2000) 765-80.

Figure 1: Furnace at Work Showing the fire front, burning chamber, door, brick in contact with thermocouples for wall temperature measurement.

JCSE The Journal of Corrosion Science and Engineering
ISSN 1466-8858 Volume 12, Preprint 14 submitted 3 May 2009

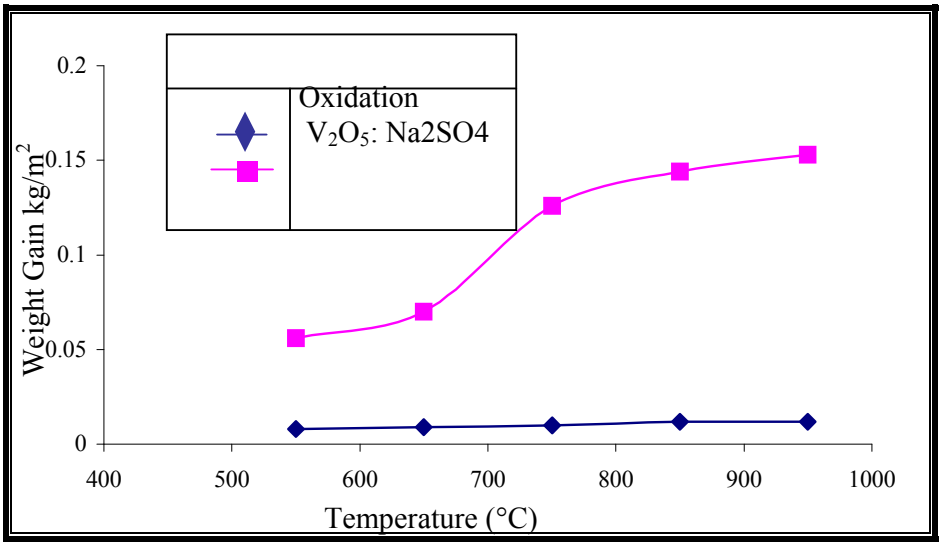

Fig. 2: Effect of heating Temperature and Weight Gain for 209 T1 Specimens at four hours of exposure.

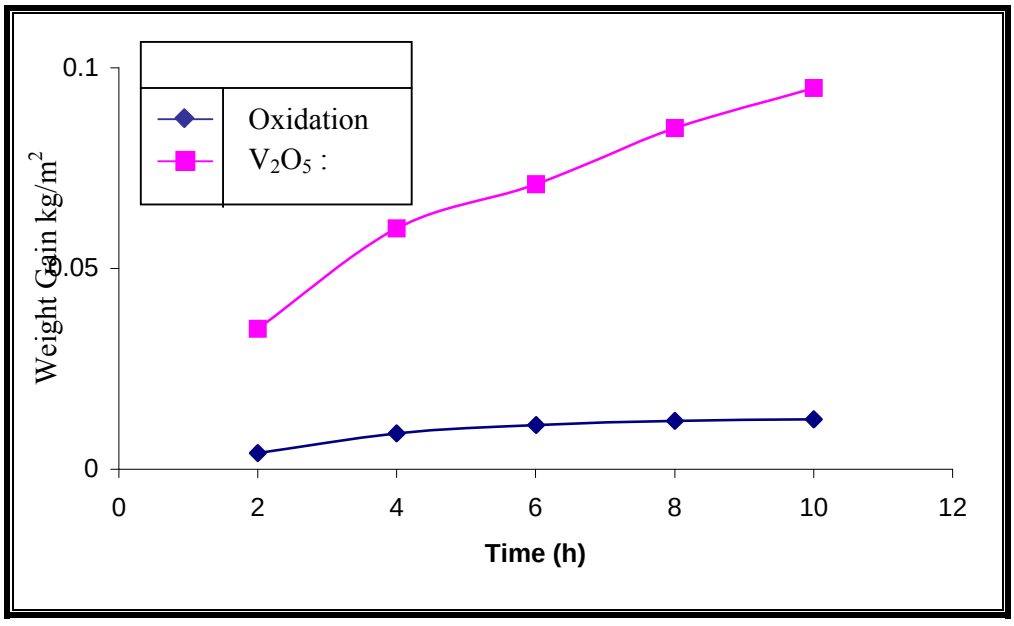

Fig. 3: Effect of exposure Time on Weight Gain for SA-178A Specimens at 550°C.

ISSN 1466-8658 Volume 12, Preprint 14 submitted 3 May 2009

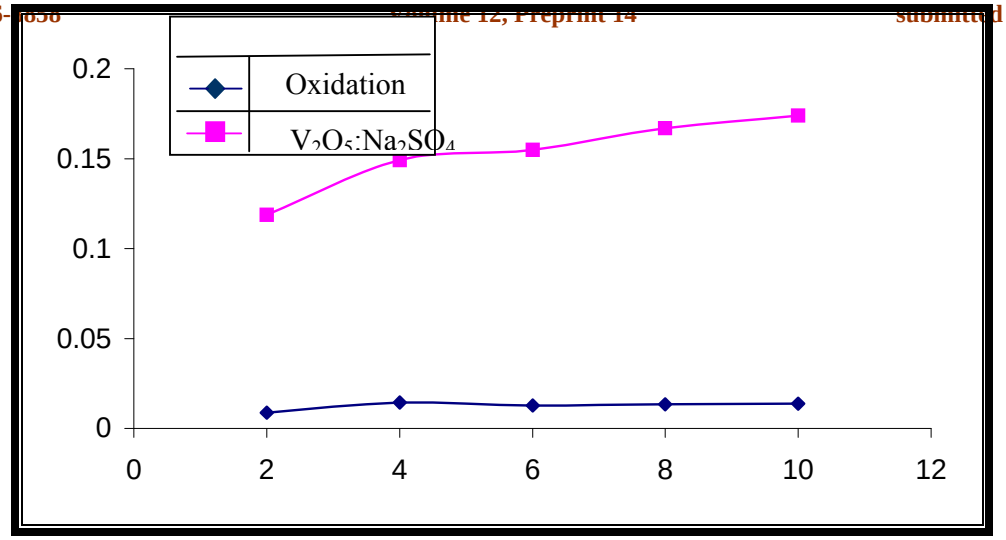

Fig.4: Effect of exposure Time on Weight Gain for (213 T11) Specimens at 950 °C.

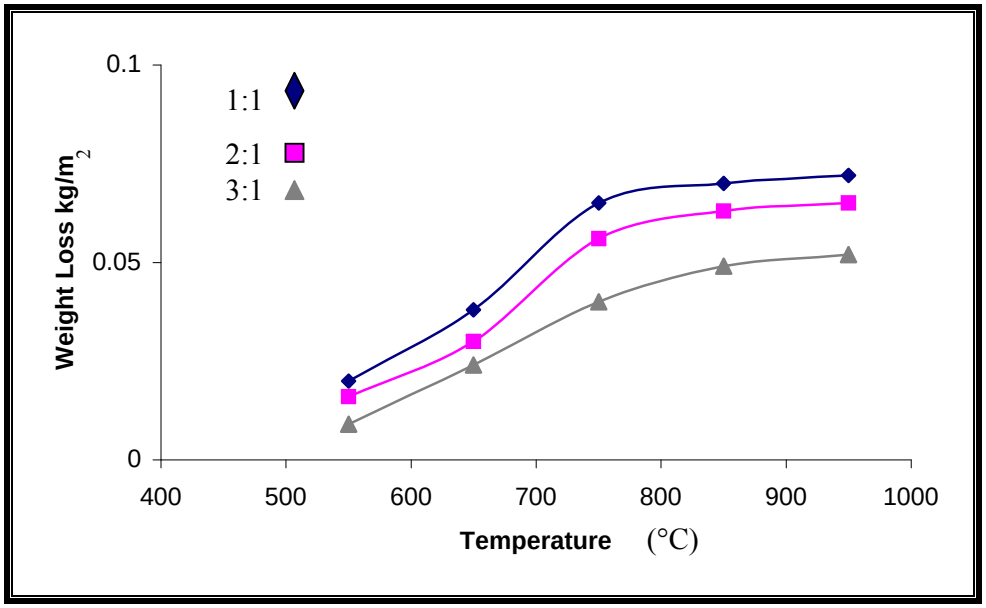

Fig. 5: Effect of Temperature on weight loss at various Ratios of $Mg(OH)_2$:Ash for SA-178A Specimens at 4h

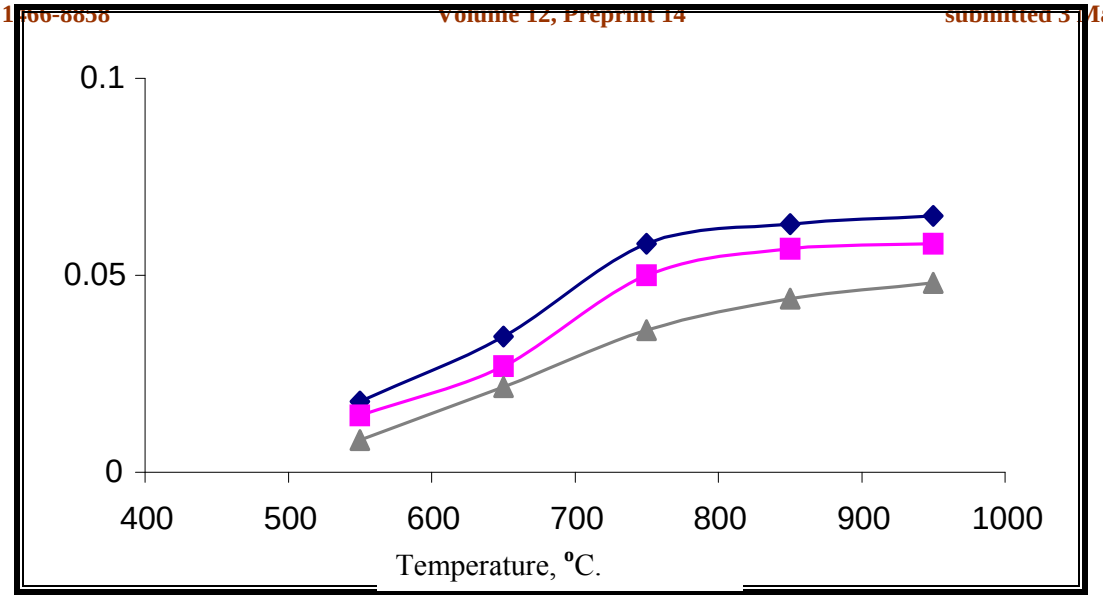

Fig. 6: Effect of Temperature on weight loss at various Ratio of $Mg(OH)_2$:Ash. For (209 T1) Specimens at (4 h)

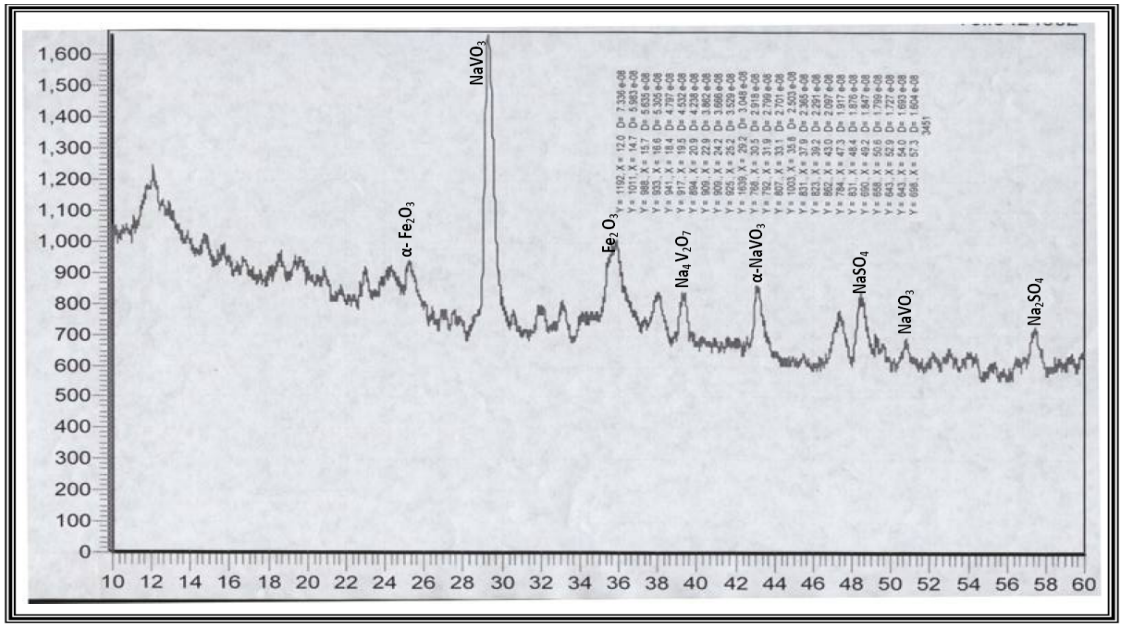

Fig. 7: X-ray Diffraction Analysis of Deposits on SA-178 Specimen Coated with Ash , Heated at 750˚C and 4h.

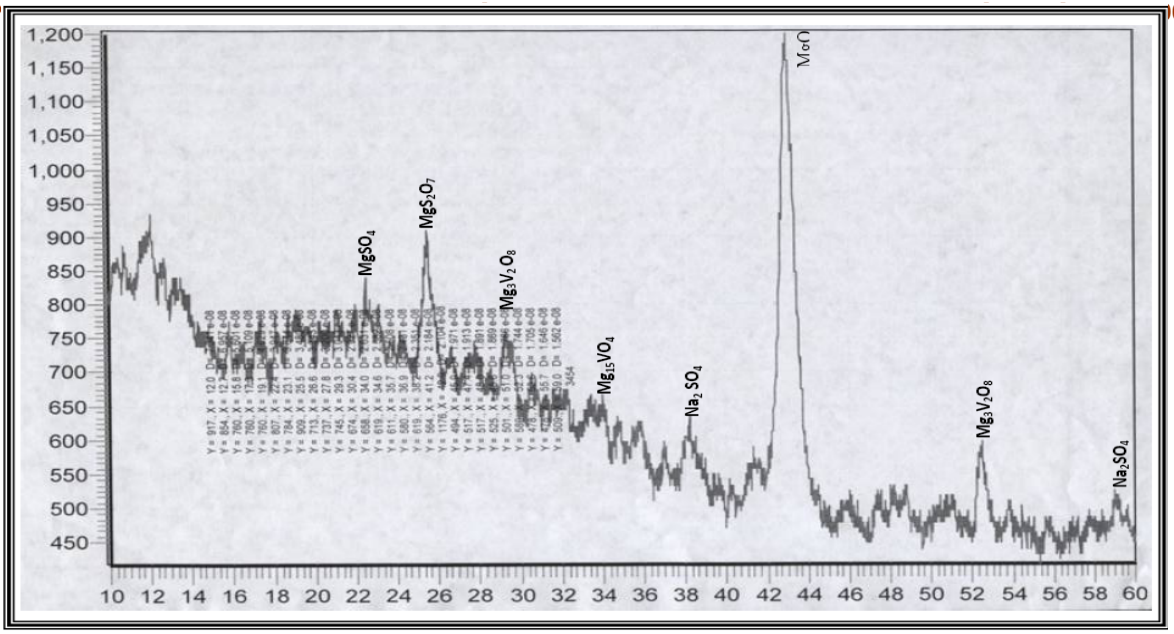

Fig. 8: X-ray Diffraction Pattern of Deposits on 213 T11 Specimen Coated with [3:1] $Mg(OH)_2$:Ash, Heated at 750˚C for 4h.

TABLE 1: Chemical Composition of Alloys [17]

Components	SA-178A%	209 T1%	213 T11%
C	0.06-0.18	0.1-0.2	0.08-0.15
Mn	0.27-0.73	0.3-0.8	0.3-0.6
Pmax.	0.035	0.025	0.025
S max.	0.035	0.025	0.025
Fe	Remain	Remain	Remain
Si		0.1-0.5	0.5-1
Mo		0.044-0.65	0.44-0.65
Cr			1-1.5

TABLE 2: Weight Losses in the Presence of $Mg(OH)_2$ for (SA-178) Specimens.

$Mg(OH)_2$:Ash	Temperature, °C.				
	550	650	750	850	950
0:1	--0.06	--0.078	--0.14	--0.16	--0.17
1:1	0.02	0.037	0.065	0.07	0.072
2:1	0.016	0.03	0.056	0.063	0.065
3:1	0.009	0.024	0.04	0.044	0.052

TABLE 3: Inhibition Efficiency in the Presence of $Mg(OH)_2$ for (SA-178) Specimens.

$Mg(OH)_2$:Ash	Temperature, °C.				
	550	650	750	850	950
0:1	--	--	--	--	--
1:1	66	51	53	56	57
2:1	73	61	60	60	62
3:1	85	69	71	69	69

a Inhibition efficiency = [(wo-wi) / wo] * 100 %

Where:Wo = weight loss in the presence of [Ash]

Wi = weight loss in the presence of [Ash + Mg $(OH)_2$]

TABLE 4: Weight Losses in the Presence of $Mg(OH)_2$ for (209 T1) Specimens.

$Mg(OH)_2$:Ash	Temperature, °C.				
	550	650	750	850	950
0:1	0.056	0.07	0.126	0.144	0.153
1:1	0.018	0.0344	0.058	0.063	0.065
2:1	0.0144	0.027	0.05	0.057	0.058
3:1	0.0081	0.0216	0.036	0.0441	0.048

TABLE 5: Inhibition Efficiency in the Presence of $Mg(OH)_2$ for (209 T1) Specimens.

$Mg(OH)_2$:Ash	Temperature, °C.				
	550	650	750	850	950
0:1	--	--	--	--	--
1:1	68	51	54	56	57
2:1	74	61	60	60	62
3:1	85	69	71	69	68

a Inhibition efficiency = [(wo-wi) / wo] * 100 %

Where:Wo = weight loss in the presence of [Ash]

Wi = weight loss in the presence of [Ash + $Mg(OH)_2$]

TABLE 6: Weight Losses in the Presence of $Mg(OH)_2$ for (213 T11) Specimens.

$Mg(OH)_2$:Ash	Temperature, °C.				
	550	650	750	850	950
0:1	0.053	0.068	0.123	0.140	0.149
1:1	0.0176	0.0325	0.057	0.0616	0.063
2:1	0.014	0.026	0.044	0.055	0.057
3:1	0.0079	0.021	0.035	0.038	0.045

TABLE 7: Inhibition Efficiency in the Presence of $Mg(OH)_2$ for (213 T11) Specimens.

	Temperature, °C.				
$Mg(OH)_2$:Ash	550	650	750	850	950
0:1	--	--	--	--	--
1:1	67	52	55	55	58
2:1	73	62	60	61	62
3:1	85	69	72	72	70

a Inhibition efficiency = [(wo-wi) / wo] * 100 %

Where:Wo = weight loss in the presence of [Ash]

Wi = weight loss in the presence of [Ash + $Mg(OH)_2$]